https://doi.org/10.1007/s41230-019-8176-9

Investigations on tribo-mechanical behaviour of Al-Si10-Mg/sugarcane bagasse ash/SiC hybrid composites

***Shankar Subramanian[1], Balaji Arunachalam[1], Kawin Nallasivam[2], Alokesh Pramanik[3]**

1. Department of Mechatronics Engineering, Kongu Engineering College, Erode - 638060, TamilNadu, India;

2. Department of Mechanical Engineering, Kongu Engineering College, Erode - 638060, TamilNadu, India;

3. School of Civil and Mechanical Engineering, Curtin University, Bentley, WA, Australia

Abstract: The effect of mechanical and tribological behaviour of aluminium alloy (Al-Si10-Mg) with sugarcane bagasse ash and silicon carbide reinforced metal matrix composites were investigated. Al-Si10-Mg alloy reinforced with 9wt.% of treated sugarcane bagasse ash particles of size (< 75 μm) and 0wt.%, 3wt.%, 6wt.% and 9wt.% of silicon carbide particles of size (< 25 μm) were fabricated using the stir casting method. Morphological analysis was done using scanning electron microscopy to access the distribution of reinforcement particles in the matrix alloy. Tensile, hardness, and impact strengths were increased with an increase in weight fraction of SiC reinforcement particles in the aluminium alloy, while the ductility was decreased. Pin-on-disc dry sliding wear test was carried out with 10, 20 and 30 N loads with a sliding speed of 10 $m \cdot s^{-1}$ for a constant time period of 20 min to predict the wear behaviour of the developed composites. Worn surfaces of the wear-tested specimens and fracture morphology structure of the tensile-tested specimens were analysed. Results show that the composites reinforced with sugarcane bagasse ash and silicon carbide particles exhibit superior wear resistance.

Key words: aluminium alloy; sugarcane bagasse ash; silicon carbide; mechanical properties; wear; fracture morphology

CLC numbers: TG146.21 **Document code:** A **Article ID:** 1672-6421(2019)04-277-08

Recently, most conventional materials are replaced with composites in various applications, due to their high stiffness, high strength, light weight and good creep resistance [1, 2]. Aluminium alloy is commonly used in the high volume casting process because it is one of the most economical materials [3] that can be used for automotive, aerospace and defence industries [4]. Several research works have been carried out to enhance the aluminium alloy properties by utilizing the various reinforcement such as SiC, B_4C, Al_2O_3, TiC, fly ash, agro waste ash, and bean pod ash, etc [5-9]. Most of the investigators [10] obtained the high wear resistance of aluminium alloy matrix composites by incorporating SiC particles as reinforcement [11]. Sugarcane bagasse is a waste by-product of the sugarcane industry during the extraction of juice from cane, and is enormously available in sugar factories. Sugarcane bagasse ash mainly contains crystalline silica-rich particles, which can be used as a reinforcement for aluminium alloy materials in order to achieve the economic production compared with other reinforcement materials such as, B_4C, Al_2O_3, TiC, etc [12]. Varieties of methods have been employed in recent years for the production of metal matrix composites including liquid metallurgy [13], liquid infiltration [14], stir casting [15], impeller mixing [16], spray deposition [17], and squeeze casting [18]. In order to achieve mass production of hybrid aluminium alloy composite materials, the stir casting process is mostly preferrable [19]. Hence, the present study has been carried out with stir casting to reinforce aluminum alloy (Al-Si10-Mg) with sugarcane bagasse ash and SiC particles.

Attempts have been made by researchers in the process of aluminium hybrid metal matrix composite (HMMC) fabrication with different reinforcement elements as well as different manufacturing methods [20-23]. SiC and fly ash reinforcement particles were uniformly disseminated in Al356/SiC/fly ash HMMC fabricated using electromagnetic casting process [24]. Powder

***Shankar Subramanian**

Male, born in 1980, Professor. His research interests are computational wear modelling – tribology, biomechanics, ergonomics and machine design. He is a life member of the Tribology Society of India, Indian Society for Technical Education, and an Associate Member of the Institute of Engineers. To date, he has published 75 technical papers in international journals.

E-mail: shankariitm@gmail.com

Received: 2018-12-20; Accepted: 2019-04-15

metallurgy process was also adopted for the uniform distribution of reinforcement particles in synthesis of hybrid nano-composite materials, and it was confirmed from SEM morphologies, XRD and wear test results [25]. A356/SiC_p/MoS_2 hybrid composites were fabricated using friction stir processing method, and the microstructure, hardness and tribological behaviour were studied [26]. The SiC_p and fly ash reinforcements, with different weight proportions, obviously improve the corrosion resistance of recycled aluminium alloy [27]. The influence of SiC particles on high strength aluminium alloys AA7010, AA7009 and AA2024 during sliding wear were studied [28] and improved wear resistance was confirmed in the developed materials. The inclusion of 15% fly ash and SiC particulates increased the tensile strength, compression strength and impact strength of the HMMCs, and further studies proved the dry sliding wear resistance also increased with the increase of reinforcement content [29].

From the above works, it can be clearly understood that the reinforcement materials SiC and fly ash influenced the tribological properties of hybrid aluminium alloy materials. To date, no research work has been carried out to study the behaviour of sugarcane bagasse ash and silicon carbide (SiC) particles as reinforcement with aluminium alloy material. The present work focused on the fabrication of aluminium alloy composite materials with Al-Si10-Mg as base material and sugarcane bagasse ash (SBA) and SiC particles as reinforcements. The tribo-mechanical behaviour of the Al-Si10-Mg/SBA/SiC hybrid composites were also investigated.

1 Methodology

1.1 Materials

Aluminium alloy Al-Si10-Mg was taken as base material and its chemical composition is listed in Table 1. It is a typical casting alloy used for parts with thin walls, subjected to high loads and complex geometry like automobile parts, aircraft parts, etc. It also offers good strength, hardness and dynamic properties. In addition to the base material, sugarcane bagasse ash and silicon carbide with the particle size of 0–75 μm and 0–25 μm, respectively, were used as reinforcements.

Table 1: Chemical composition of Al-Si10-Mg alloy (%)

Cu	Mg	Si	Fe	Mn	Ni	Zn	Pb	Sn	Ti	Al
0.1 Max.	0.2–0.6	10–13	0.6 Max.	0.3–0.7	0.1 Max.	0.1 Max.	0.1 Max.	0.2 Max.	0.005 Max.	Bal.

1.2 Sugarcane bagasse ash

Sugarcane bagasse is the fibrous substance that remains after sugarcane stalks are crushed to extract their juice. The abundantly available sugarcane bagasse was collected from the local sugar mill and it was cleaned thoroughly with water to remove any foreign elements. Then the bagasse was dried in sunlight for 2 to 3 days and then crushed into small pieces. The crushed pieces were dispensed in the electric furnace container and heated at 300 ºC for 3 to 4 h to get black colour ash, as shown in Fig. 1(a). By using a normal sieve, the combusted sugarcane ashes were filtered and then being heated in the electric furnace for 12 h at 1,200 ºC to obtain the greyish white colour ash, as shown in Fig. 1(b). The greyish white sugarcane bagasse ashes were filtered in the size of 75 μm by using the test sieve. The EDAX and SEM microstructure tests were carried out to ensure the availability of sufficient silicon in the fabricated whitish ashes, as shown in Fig. 2 and Fig. 3, respectively [25]. The EDAX test composition results for the fabricated sugarcane bagasse ash are shown in Table 2.

1.3 Silicon carbide

Silicon carbide (SiC) was produced by the carbothermal reduction of silica in an electric furnace. During the process, silicon carbide became a very fine residue or fine united lumps which were crushed and powdered to yield a functional raw material. The properties of SiC particles are listed in Table 3.

(a) Raw ash at room temperature (b) Greyish white ash after heated at 1,200 ºC

Fig. 1: Preparation of sugarcane bagasse ash

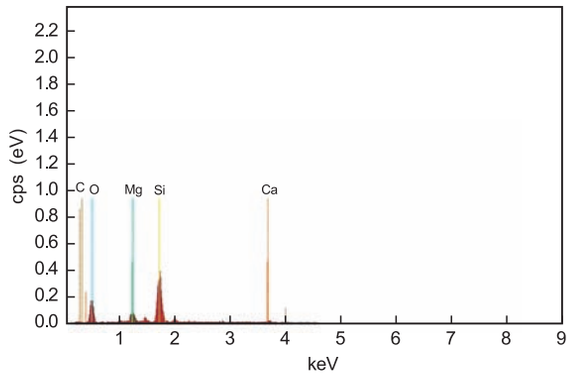

Fig. 2: EDAX micrograph of sugarcane bagasse ash [25]

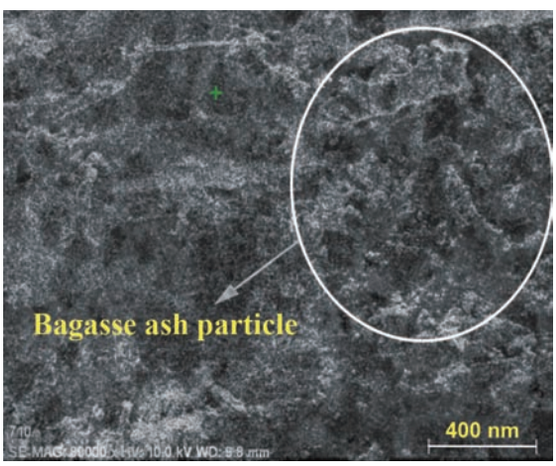

Fig. 3: SEM micrograph of sugarcane bagasse ash [25]

Table 2: Chemical composition of sugarcane bagasse ash (%)

Si	O	Ca	Mg
41.19	41.90	9.08	7.83

Table 3: Properties of SiC particles

Properties	Values
Melting point	2,200–2,700 ºC
Vickers hardness	2,800–3,300
Density (g·cm^{-3})	3.2
Crystal structure	Hexagonal

2 Experimental procedure

The liquid metallurgy method was adopted to fabricate the aluminium matrix composite. Stir casting technique was employed to prepare the aluminium alloy reinforced with sugarcane bagasse ash and SiC. Firstly, the Al-Si10-Mg alloy was charged into the graphite crucible furnace at 650 ºC. Then, the mixture of sugarcane bagasse ash and SiC was added (1–2 g per stoke of stirring) into the melted alloy. The reinforcement particles were preheated to 800 ºC for 1 h before being added into the melt. The stainless steel stirrer was rotated at 500–700 rpm during the mixing process. About 30 g of degassing agent hexachloroethane (C_2Cl_6) were added in the furnace to remove the internal voids. Concurrently, 1wt.% of magnesium was added into the molten mixture to improve the wettability between the aluminium alloy and reinforcement particles. To achieve the uniform distribution of reinforcement particles, the stirring process was continued for 5–10 min. The distribution of sugarcane bagasse ash and SiC particles were analyzed using scanning electron microscopy (SEM) micrographs. Four specimens were fabricated with four different weight percentages of SiC (0%, 3%, 6%, 9%) and a constant weight of 9% sugarcane bagasse ash particles, as shown in Table 4.

Table 4: Composition of reinforcement

Sample No.	Composition of reinforcement	SiC (wt.%)
1	Al-Si10-Mg + 9% SBA ash	0
2	Al-Si10-Mg + 9% SBA ash	3
3	Al-Si10-Mg + 9% SBA ash	6
4	Al-Si10-Mg + 9% SBA ash	9

2.1 Tribological test

A pin-on-disc tribometer was utilized to assess the friction and wear behaviour corresponding to the sliding contact surface of the prepared sample. A test specimen with the size of 6 mm in diameter and 25 mm in height was prepared from each cast alloy using EDM wire cutting machine for the wear test. The faces of the specimen were polished using a metal disc polishing machine to attain the uniform wear, as shown in Fig. 4(a). Wear study was carried out under a moisture free environment and sliding circumstances were set as per ASTM standard G99-05. High hardness steel of 58–60 HRC was used as the disc material for the pin on disc tribometer. Surface roughness of the steel disc was 0.5 μm with dimensions of 165 mm in diameter and 8 mm in thickness. The chemical compositions of steel disc are carbon, silicon, manganese, sulphur and phosphorus. Experimental wear tests were done at different loading conditions of 10, 20 and 30 N, and sliding speed of 10 m·s^{-1} for 20 min at a sliding interval of 2,413 m. The tracking diameter maintained at 110 mm throughout the test. The wear rates of the hybrid composite specimens were calculated by weight loss method. The worn out surfaces were analyzed using a high resolution scanning electron microscope.

2.2 Mechanical test

The following mechanical tests were carried out:

(1) The tensile test was carried out on a universal testing machine. The dimensions of the tensile test specimen were as per ASTM: E8 standards. The specimen had a gauge length of 25 mm from the total length of 100 mm, as shown in Fig. 4(b).

(2) Impact strength was assessed using a Charpy impact test. The specimen was prepared as per ASTM: E2248 standards, i.e., 10 mm ×10 mm dimensions, as shown in Fig. 4(c).

(3) The hardness test was carried out on a Brinell hardness tester under a load of 187.5 kg with a dwelling time of 20 s.

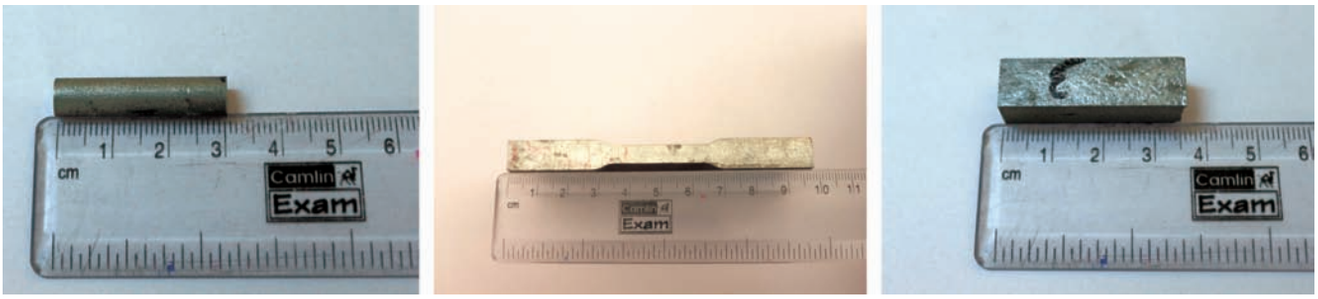

(a) Wear specimen (b) Tensile test specimen (c) Impact specimen

Fig. 4: Specimens for tribological test

(4) The ductility test was carried out on a universal testing machine to measure the percentage of elongation of composites before the rupture stage.

3 Results and discussion

3.1 Microstructure analysis

Figures 5 (a) – (c) show the morphological structure of the SBA and SiC reinforced Al-Si10-Mg aluminium alloy composites. The microstructure confirms the presence of minimal voids and slag in the developed composites and also reveals the presence of sugarcane bagasse ash and SiC particle reinforcements. At the same time, the uniform distribution of reinforcement particles in the matrix was observed. This was achieved from proper stirring in the stir casting process during the fabrication of composites, which avoids the air interference during the addition of SiC and SBA reinforcement particles in the molten metal. The stir casting process plays a major role in the distribution of reinforcement particles in the matrix alloy and helps to avoid the voids in the fabricated composites [30].

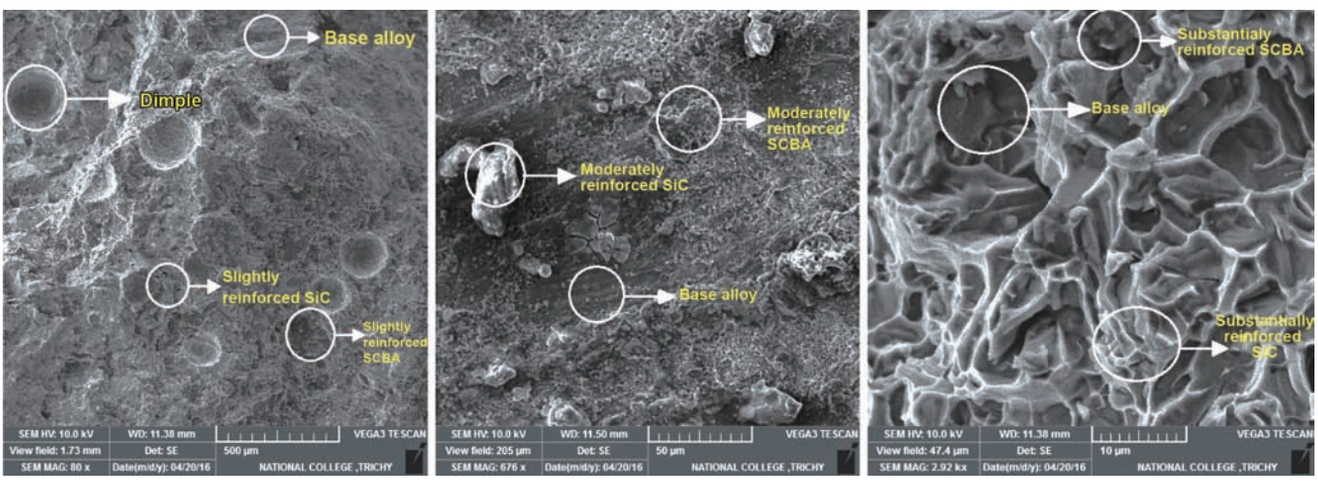

(a) 3% SiC + 9% SBA (b) 6% SiC + 9% SBA (c) 9% SiC + 9% SBA

Fig. 5: SEM micrographs for distribution of ash and SiC particles

3.2 Effect of reinforcement and load on wear rate

The tribological study was carried out with three different loads for all samples, and the values were plotted in the graph. Figure 6 shows the effect of varying load conditions on wear rate of composites reinforced with different weight fractions of SiC and SBA particles. It can be seen that an increase in the content of SiC particles decreases the wear rate of the composites, but an increase in load value increases the wear amount of the developed composites. During sliding, the reinforcement particles formed a thick tribo layer between the contact surfaces. At lower loads, these layers form as a third body component between the contact surfaces, thus increasing the wear resistance. At higher loads, these layers get broken down, resulting in high wear rate and high coefficient of friction (COF). Similar

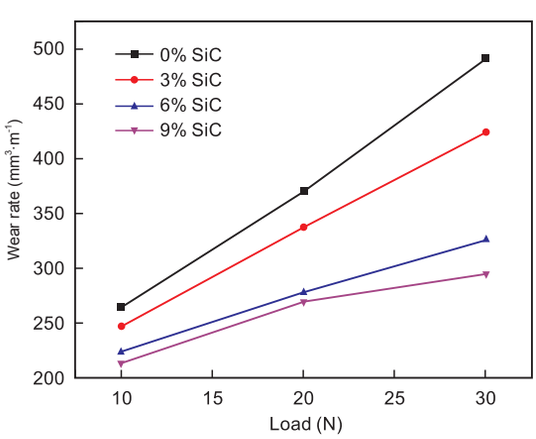

Fig. 6: Effect of reinforcement and load on wear rate

conclusions were made in AA6351-SiC-B_4C HMMCs in which the addition of SiC and B_4C particles creates a thick tribo layer and boron oxide layer respectively, between the contact surfaces during sliding conditions, which enhanced the wear resistance [31].

3.3 Effect of load on coefficient of friction (COF)

The variation of coefficient of friction with load for the developed composites with different weight fractions of reinforcements were studied, as shown in Fig. 7. It shows that the increase in reinforcement content decreases the friction coefficient of the developed composites and vice versa. Sample 4 with 10 N load shows the lowest COF, whereas Sample 1 with 30 N load has the highest COF. Also, an increase in load increases the frictional force during the pin-on-disc process which implies the high COF value. It was concluded that the composite with 3wt.% SiC has a high COF with rough surfaces and the composite with 9wt.% SiC has a low COF with smooth surfaces, as shown in Fig. 8. Similar observations were given in HMMCs [31, 32]; it was reported that the increase in SiC reinforcements decreases the COF of the aluminum metal matrix composite [33].

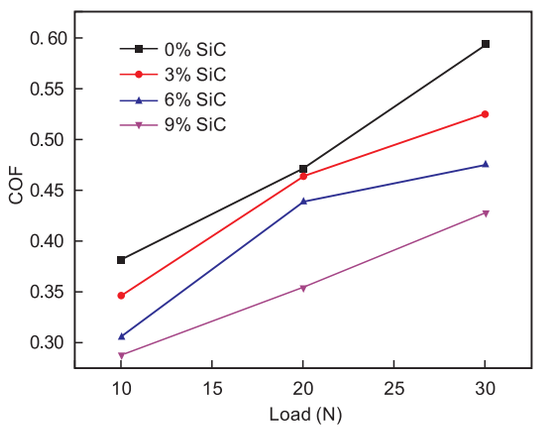

Fig. 7: Effect of reinforcement and load on COF

3.4 Worn morphology of composite

The surface morphology of the worn surfaces is shown in Fig. 8. During the sliding operation, predominantly, adhesive wear mechanism was observed in the developed composites, which was ensured by the formation of wear fragments. It is clearly evidenced that Fig. 8(a) shows an abraded surface which contains grooves and higher wear debris and Figs. 8 (b) and (c) show a smooth surface during wear track in the longitudinal direction. The oxide layer formation was observed in Fig. 8(c) which acts as a third body component during the sliding, and the flake shape wear debris was formed. The oxide layer forms as a protective silica layer over the fabricated aluminium composite at higher tempertatures. Similar observations were identified in the HMMCs worn morphological study [34]-[35]. Therefore, it was concluded that the formation of grooves and cracks on the composite decreases when increasing the weight percentage of SiC reinforcement.

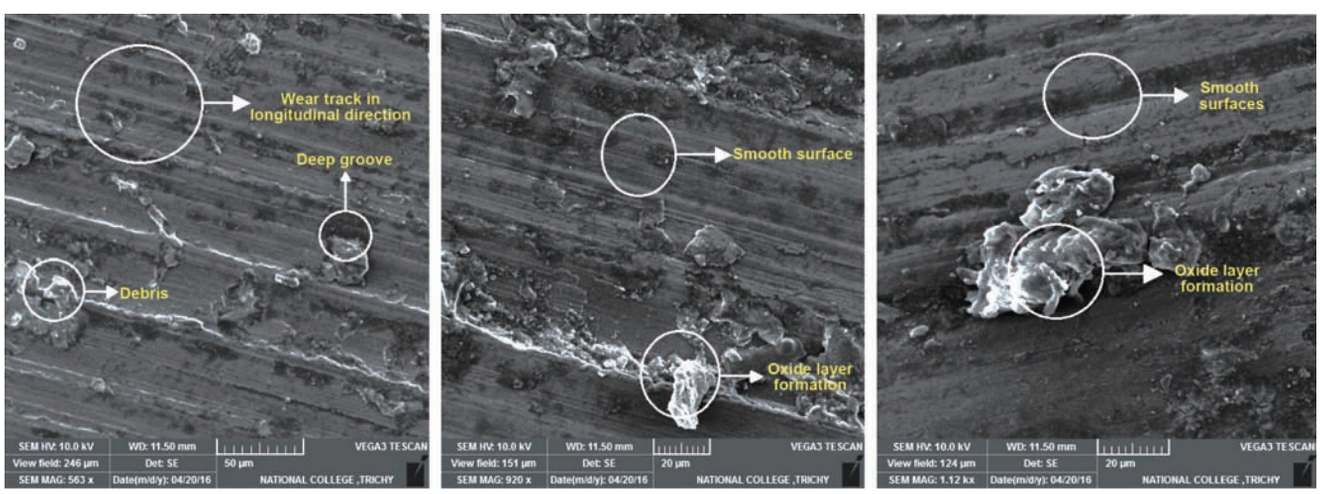

(a) 3% SiC + 9% SBA (b) 6% SiC + 9% SBA (c) 9% SiC + 9% SBA

Fig. 8: SEM worn surface morphology

3.5 Tensile behaviour

Figure 9 shows the variation of the tensile strength of Al-Si10-Mg/SBA/SiC composites with different weight fractions of reinforcement particles. The ultimate tensile strength increases with the increase of reinforcement particles (SBA and SiC). It increases from 138.92 MPa (Sample 1) to 161.73 MPa (Sample 4) by increasing the SiC reinforcement from 0% to 9% with a constant 9wt.% SBA. The tensile strength of Samples 2, 3 and 4 increased by 5.7%, 10.9% and 16.5%, respectively, compared to the Sample 1 with 0wt.% of SiC. The greatest tensile strength was observed as 161.73 MPa for the composite (Al-Si10-Mg alloy+9% SiC+9% SBA), which was 26.3 % higher than the base alloy Al-Si10-Mg [25]. The increase in weight percentage of the reinforcement increases the tensile strength of the composites due to the homogeneous distribution of reinforcement particles in the composites. Similar results were observed in literature [36].

3.6 Impact strength

Figure 10 indicates the variation of impact strength of Al-Si10-Mg/SBA/SiC composites with the weight fraction of SiC reinforcements at constant 9% SBA. The impact strength of

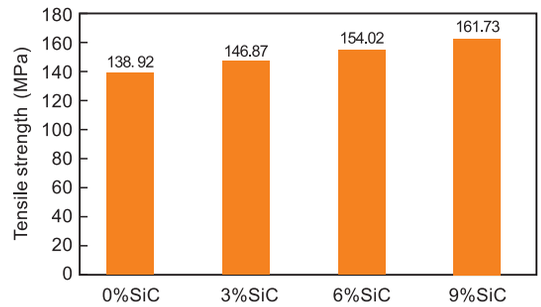

Fig. 9: Variation of tensile strength with weight fraction of SiC reinforcement particles (with constant 9% SBA)

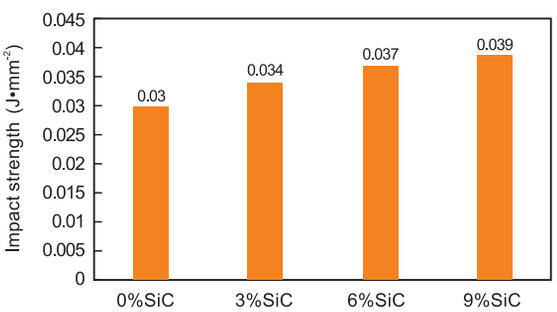

Fig. 10: Variation of impact strength with weight fraction of SiC reinforcement particles (with constant 9% SBA)

the developed composite was increased from 0.03 (Sample 1) to 0.039 J·mm^{-2} (Sample 4), i.e., impact strength of Sample 4 was increased by 14.2% compared to Sample 1 while increasing the SiC reinforcement from 0wt.% to 9wt.%. This high impact strength was achieved due to the strong interfacial bonding between the reinforcement (SBA and SiC) particles and aluminium alloy. Similiar results were found in the HMMCs where the SiC and fly ash particles were utilized as reinforcements [36]. This investigation implies that the impact strength of the developed composites increased due to the increase of SiC reinforcements.

3.7 Hardness

Figure 11 shows the variation of hardness, which was increased with the increase of reinforced particles. The hardness of (Al-Si10-Mg + 9wt.% SBA) composite increased from 102.69 BHN to 129.76 BHN, improved by 14.5%, while increasing the SiC particles from 0 to 9wt.%. The presence of hard particles of reinforcement provided more resistance to plastic deformation which leads to an increase in hardness of the aluminium alloy. This improvement proves the fact that the SiC possesses higher hardness and its presence in the matrix improves the hardness of the composites. Similar observations were reported earlier in AA6061/fly ash composites, where the hardness was increased by 67% while increasing the SiC particle up to 6% [10]. Hence, the hardness of the developed composites mainly depends upon the increase of reinforcement particles in the matrix material.

3.8 Percentage of elongation

The ductile behaviour of the fabricated composite specimens

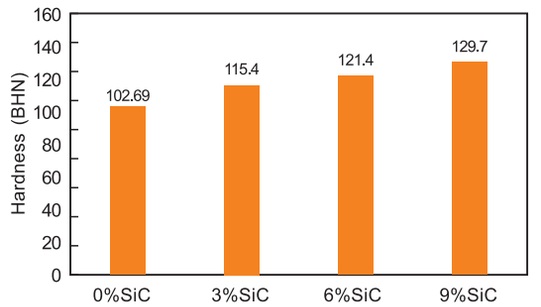

Fig. 11: Variation of hardness with weight fraction of SiC reinforcement particles (with constant 9% SBA)

was estimated in terms of maximum percentage of elongation. Figure 12 shows a decrease in elongation while increasing the content of reinforcements. The percentage of elongation was decreased from 2.61 to 2.13, decreased by 13.2%, due to the increase of SiC reinforcement from 0wt.% to 9wt.%. The fine grains of sugarcane bagasse ash and SiC particles provided good bonding between the aluminium alloy matrix and reinforcement particles, which decreased the percentage of elongation of the composite. The ductility of Al6061-SiC composites [37] and Al356/SiC/fly-ash hybrid composites [10] was decreased significantly due to the addition of SiC particles with similar findings as this work.

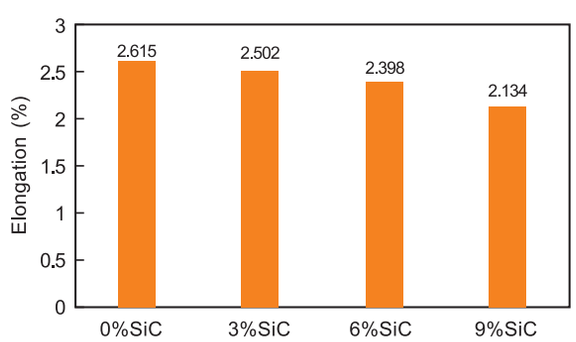

Fig. 12: Variation of elongation with weight fraction of SiC reinforcement particles (with constant 9% SBA)

3.9 Fracture morphology

Morphological structure of the tensile tested fracture specimen is shown in Fig. 13, which reveals the homogeneous distribution of reinforcement particles. Some voids and propagated crack paths are visible under tensile loading in Fig. 13(b), which ensures the ductile fracture occurred in the 6wt.% of SiC reinforced composite. The fractured surface of the 9wt.% SiC reinforced composite shown in Fig. 13(c), has fewer voids and cracks than the 6wt.% SiC reinforced specimen. Higher magnification image shows the good bonding between the aluminium alloy and reinforcement particles, and the elliptical shape well bonded particles were highly collapsed and elongated after tensile loading. The elliptical shape was formed due to the reasonable clustering of fine grains of silicon particles in the aluminium alloy matrix and reinforcement particles. The collapsed and evident elongated elliptical shape reveals the

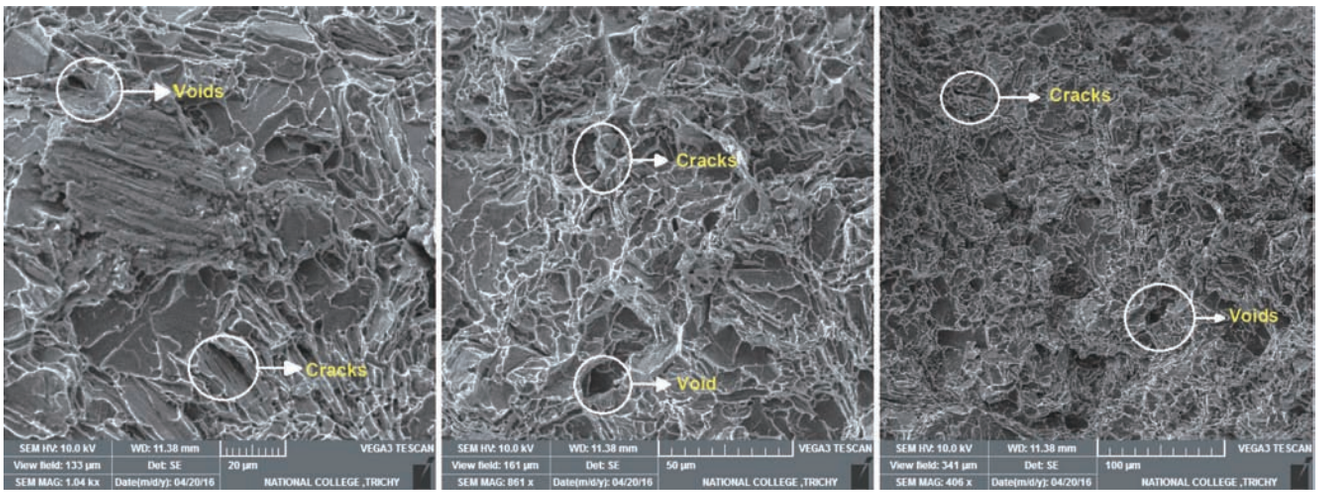

(a) 3% of SiC + 9% of SBA (b) 6% of SiC + 9% of SBA (c) 9% of SiC + 9% of SBA

Fig. 13: Fractured morphology of tensile specimens

presence of crack propagation in the composite and also denoted the presence of fewer voids in the fabricated alloy. A similar morphological structure was obtained in the tensile tested fracture aluminium alloy-alumina-boron carbide metal matrix composite specimen [36]. From the fractographic analysis, it was determined that the increase of reinforcement particles in the base matrix alloy results in better resisting properties.

4 Conclusions

Hybrid metal matrix composites Al-Si10-Mg/sugarcane bagasse ash/SiC were fabricated using the stir casting method with four different weight percentages of SiC particles (0wt.%, 3wt.%, 6wt.% and 9wt.%) with constant 9wt.% SBA. The following conclusions from the experiments were obtained:

(1) Scanning electron microscopy images confirmed the homogeneous distribution of reinforcement particles in the aluminium alloy. The worn surface morphology shows the crack formation and wear debris formation in the fabricated alloy while increasing the load.

(2) The tribological tests were conducted for the four samples with three different loads (10, 20, and 30 N), with constant speed and sliding distance. The lower wear rate and coefficient of friction are observed in Sample 4 (Al-Si10-Mg+9% SiC+9% SBA) with 10 N load.

(3) The mechanical properties such as tensile strength, impact strength and hardness of the fabricated composites increase while increasing the content of SiC. Meanwhile, the ductility value decreases due to the increasing content of SiC. An increase in the addition of SiC to 9% in the base aluminium alloy Al-Si10-Mg increases the tensile strength by 16.5%, impact strength by 14.2%, hardness by 14.5%, and decreases the ductile strength by 15.2% compared to the composite Al-Si10-Mg alloy without SiC.

(4) The results indicate that the SBA and SiC were the suitable combination of reinforcments in the AlSi10Mg composites, and also, that the reinforcement particles do not degrade the mechanical and tribological properties of the base AlSi10Mg alloy.

References

[1] Danels D. Analysis of Stress-Strain, Fracture and Ductility Behaviour of Aluminium Matrix Composites Containing Discontinuous Silicon Carbide Reinforcement. Metall. Trans, 1985, 16: 1105–1115.

[2] Wong C S, Pramanik A, and Basak A. Residual stress generation in metal matrix composites after cooling. Materials Science and Technology, 2018, 34: 1–13.

[3] Kumar P, Kumaran S, Rao T S, et al. High temperature sliding wear behavior of press-extruded AA6061/fly ash composite. Materials Science and Engineering: A, 2010, 527(6): 1501–1509.

[4] Prasad S, and Asthana R. Aluminum metal-matrix composites for automotive applications: tribological considerations. Tribology Letters, 2004, 17(3): 445–453.

[5] Pramanik A. Effects of reinforcement on wear resistance of aluminum matrix composites. Transactions of Nonferrous Metals Society of China, 2016, 26(2): 348–358.

[6] Aigbodion V, Atuanya C, Edokpia R, et al. Experimental study on the wear behaviour of Al-Cu-Mg/bean pod ash nano-particles composites. Transactions of the Indian Institute of Metals, 2016, 69(4): 971–977.

[7] Rao R G, Sahoo K, Ganguly R. Effect of Flyash Treatment on the Properties of Al-6061 Alloy Reinforced with SiC-Al_2O_3-C Mixture. Transactions of the Indian Institute of Metals, 2017, 70(10): 2707–2717.

[8] Paknia A, Pramanik A, Dixit A, et al. Effect of size, content and shape of reinforcements on the behavior of metal matrix composites (MMCs) under tension. Journal of Materials Engineering and Performance, 2016, 25(10): 4444–4459.

[9] Pramanik A, and Basak A K. Effect of machining parameters on deformation behaviour of Al-based metal matrix composites under tension. Proceedings of the Institution of Mechanical Engineers, Part B: Journal of Engineering Manufacture, 2018, 232(2): 217–225.

[10] Manna A, and Bhattacharayya B. A study on machinability of Al/SiC-MMC. Journal of Materials Processing Technology, 2003, 140(1-3): 711–716.

[11] Hakami F, Pramanik A, and Basak A K. Tool wear and surface quality of metal matrix composites due to machining: A review. Journal of Engineering Manufacture, 2017, 231(5): 739–752.

[12] Faria K, Gurgel R, and Holanda J. Recycling of sugarcane bagasse ash waste in the production of clay bricks. Journal of Environmental Management, 2012, 101: 7–12, 2012.

[13] Ma Y and Langdon T G. Creep behavior of an Al-6061 metal matrix composite produced by liquid metallurgy processing. Materials Science and Engineering: A, 1997, 230(1–2): 183–187.
[14] Amateau M. Progress in the development of graphite-aluminum composites using liquid infiltration technology. Journal of Composite Materials, 1976, 10(4): 279–296.
[15] Jose J, Peter E P, Feby J A, et al. Manufacture and characterization of a novel agro-waste based low cost metal matrix composite (MMC) by compocasting. Materials Research Express, 2018.
[16] Sarkar S, Sen S, Mishra S, et al. Studies on aluminum – fly-ash composite produced by impeller mixing. Journal of Reinforced Plastics and Composites, 2010, 29(1): 144–148.
[17] Mathur P, Apelian D, and Lawley A. Analysis of the spray deposition process. Acta Metallurgica, 1989, 37(2): 429–443.
[18] Ghomashchi M, and Vikhrov A. Squeeze casting: an overview. Journal of Materials Processing Technology, 2000, 101(1–3): 1–9.
[19] Yeh N M, and Krempl E. The influence of cool-down temperature histories on the residual stresses in fibrous metal-matrix composites. Journal of Composite Materials, 1993, 27(10): 973–995.
[20] Radhika N, Subramanian R, Venkat Prasat S, et al. Dry sliding wear behaviour of aluminium/alumina/graphite hybrid metal matrix composites. Industrial Lubrication and Tribology, 2012, 64(6): 359–366.
[21] Tisza M, Budai D, Kovács P, et al. Investigation of the formability of aluminium alloys at elevated temperatures. Materials Science and Engineering, 2016, doi: 10.1088/1757-899X/159/1/012012.
[22] Vencl A, Bobic I, and Stojanovic B. Tribological properties of A356 Al-Si alloy composites under dry sliding conditions. Industrial Lubrication and Tribology, 2014, 66(1): 66–74.
[23] Venkat P S, and Subramanian R. Tribological properties of AlSi10Mg/fly ash/graphite hybrid metal matrix composites. Industrial Lubrication and Tribology, 2013, 65(6): 399–408.
[24] Dwivedi S P, Sharma S, and Mishra R K. Microstructure and mechanical behavior of A356/SiC/Fly-ash hybrid composites produced by electromagnetic stir casting. Journal of the Brazilian Society of Mechanical Sciences and Engineering, 2015, 37(1): 57–67.
[25] Shankar S, Balaji A, and Kawin N. Investigations on mechanical and tribological properties of Al-Si10-Mg alloy/sugarcane bagasse ash particulate composites. Particulate Science and Technology, 2018, 36(6): 762–770.
[26] Alidokht S, Abdollah-Zadeh A, Soleymani S, et al. Microstructure and tribological performance of an aluminium alloy based hybrid composite produced by friction stir processing. Materials & Design, 2011, 32(5): 2727–2733.
[27] Pech-Canul M, Escalera-Lozano R, Pech-Canul M, et al. Degradation processes in Al/SiC_p/$MgAl_2O_4$ composites prepared from recycled aluminum with fly ash and rice hull ash. Materials and Corrosion, 2007, 58(11): 833–840.
[28] Rao R, and Das S. Effect of matrix alloy and influence of SiC particle on the sliding wear characteristics of aluminium alloy composites. Materials & Design, 2010, 31(3): 1200–1207.
[29] Mahendra K, and Radhakrishna K. Characterization of stir cast Al-Cu-(fly ash+SiC) hybrid metal matrix composites. Journal of Composite Materials, 2010, 44(8): 989–1005.
[30] Wang N, Wang Z, and Weatherly G C. Formation of magnesium aluminate (spinel) in cast SiC particulate-reinforced Al (A356) metal matrix composites. Metallurgical Transactions A, 1992, 23(5): 1423–1430.
[31] Kumaran S T and Uthayakumar M. Investigation on the dry sliding friction and wear behavior of AA6351-SiC-B4C hybrid metal matrix composites. Journal of Engineering Tribology, 2014, 228(3): 332–338.
[32] Savaşkan T, and Bican O. Dry sliding friction and wear properties of Al-25Zn-3Cu-(0–5) Si alloys in the as-cast and heat-treated conditions. Tribology Letters, 2010, 40(3): 327–336.
[33] Ahamed H, and Senthilkumar V. Role of nano-size reinforcement and milling on the synthesis of nano-crystalline aluminium alloy composites by mechanical alloying. Journal of Alloys and Compounds, 2010, 505(2): 772–782.
[34] Babu K V, Jappes J W, Rajan T, et al. Dry sliding wear studies on SiC reinforced functionally graded aluminium matrix composites. Journal of Materials: Design and Applications, 2016, 230(1): 182–189.
[35] Shen Y, Liu Y, Zhang Y, et al. Determining the energy distribution during electric discharge machining of Ti-6Al-4V. The International Journal of Advanced Manufacturing Technology, 2014, 70(1–4): 11–17.
[36] Kumar G V, Rao C, and Selvaraj N. Studies on mechanical and dry sliding wear of Al6061-SiC composites. Composites, Part B: Engineering, 2012, 43(3): 1185-1191.
[37] Murthy I N, Rao D V, and Rao J B. Microstructure and mechanical properties of aluminum–fly ash nano composites made by ultrasonic method. Materials & Design, 2012, 35: 55–65.